Engineering Structures 95 (2015) 138–153

Contents lists available at ScienceDirect

Engineering Structures

journal homepage: www.elsevier.com/locate/engstruct

Assessment of seismic design parameters of moment resisting RC braced frames with metallic fuses

A. Tena-Colunga [a,*], H.J. Nangullasmú-Hernández [b]

[a] Departamento de Materiales, Universidad Autónoma Metropolitana, Edificio P4, Último Piso, Av. San Pablo 180, Col. Reynosa Tamaulipas, 02200 México, D.F., Mexico
[b] Posgrado en Ingeniería Estructural, Universidad Autónoma Metropolitana, Edificio P4, Segundo Piso, Av. San Pablo 180, Col. Reynosa Tamaulipas, 02200 México, D.F., Mexico

ARTICLE INFO

Article history:
Received 26 April 2014
Revised 16 March 2015
Accepted 28 March 2015
Available online 11 April 2015

Keywords:
Energy dissipation
Metallic fuses
Stiffness balances
Ductility demands
Seismic response factors
Overstrength
Design drifts
Deformation capacity

ABSTRACT

A parametric study was devoted to evaluate, using static nonlinear analyses (pushover), global seismic design parameters for low to medium rise regular reinforced concrete moment-resisting braced frames (RC-MRBFs) with hysteretic energy dissipation devices mounted on chevron steel bracing. Frame models with range from five to twenty five stories were designed using different elastic stiffness ratios between the moment frame system and the whole structure (frame-bracing-hysteretic device system). Also, different elastic stiffness balances between the hysteretic device and the supporting braces were considered. Different post to pre yielding stiffness ratios for the hysteretic devices were considered. Two angles of inclination of the chevron braces with respect to the horizontal axis were considered, taking into account typical story heights and bay widths used in Mexican practice. From the results obtained in this study, stiffness balances are defined to achieve a suitable mechanism where the hysteretic devices yield first and develop their maximum local displacement ductility, whereas in the moment frame incipient yielding is only formed at the beam ends. Finally, additional comments are made with respect to: (a) relations between global ductility capacity and local displacement ductility capacity for the hysteretic devices for a given combination of the studied stiffness parameters and angles of inclination, (b) story drifts at yielding and their relation with the selected elastic stiffness ratio between the moment frame system and the whole structure and, (c) overstrength factors for design purposes.

1. Introduction

Mexican practicing engineers and researchers have been more interested in hysteretic passive energy dissipation devices (HEDD) since 1985, as this technology was considered as one of the viable options for the seismic retrofit of some damaged buildings during the September 19, 1985 Michoacán Earthquake. It was also considered as an attractive structural system for new buildings.

Several research studies have been conducted in Mexico ever since which are summarized elsewhere [1]. However, even today there are few studies available in the literature (Mexican and worldwide) focused on defining global design parameters that could be easily included in a traditional seismic building code format such as those found in Mexican Codes such as Mexicós Federal District Code [2], the Manual of Civil Works [3,4] or US recommendations such as ASCE-7 [5]. Most of the research studies devoted to assess global seismic design parameters were conducted in highly idealized single degree of freedom systems (SDOFs) [6–10] or in SDOFs calibrated in idealized multi-degree of freedom systems (MDOFs) [11–20]. Many of these studies have been interested in validating equivalent design procedures for structures with HEDD using a supplemental viscous damping approach [6,7,10,14,16,17,21–23] and/or the FEMA-273 [24] and FEMA-274 [25] displacement-based design procedures [16,17,23]. It is beyond the scope of this paper to discuss previous design methods already reported in the literature (strong points and advantages, weaknesses and limitations), as the interested reader could find already excellent documents on this topic [14,16,17,23].

For the objectives and goals of the research which is being presented, the work conducted by Vargas and Bruneau [18–20] is worth mentioning, as they related the design base shear to the elastic stiffness ratio between the bracing-hysteretic device system and the moment frame system (α) and the maximum local displacement ductility (μ_d) for the hysteretic energy dissipation device that insures an elastic behavior for the frame. In addition, they assessed the overstrength factor for the system (Ω) related to the yielding of the energy dissipation devices before the frame

* Corresponding author. Tel.: +52 55 5318 9460; fax: +52 55 5318 9085.
E-mail addresses: atc@correo.azc.uam.mx (A. Tena-Colunga), hnangu@hotmail.com (H.J. Nangullasmú-Hernández).

http://dx.doi.org/10.1016/j.engstruct.2015.03.062
0141-0296/

undergoes inelastic deformations. Based upon their parametric study, Vargas and Bruneau [19] proposed a design procedure for MDOFs. This procedure was calibrated with the design of a three-story, one-bay frame with buckling-restrained braces (BRBs) as energy dissipation devices, which it was later built and tested in a shaking table. The obtained experimental results mostly validated the proposed design procedure.

Certainly, the research study presented by Vargas and Bruneau [18–20] is very valuable and constitutes a big step forward to adapt rational design procedures to the most widely accepted design philosophy of most seismic building codes worldwide for MRFs with HEDD, by defining global seismic reduction parameters for the design spectra, such as ductility and overstrength force reduction factors. However, as the parametric study was conducted on idealized SDOFs, there are still uncertainties on how general the applicability of the recommended design parameters could be for more complex MDOFs, for example, multi-story, multi-bay frames where many bays would not have energy dissipation devices, that it is a common structural system of interest for the design practice.

Therefore, in this paper the authors summarize the results of a parametric study devoted to evaluate, using static nonlinear analyses (pushover), the seismic behavior of low to medium rise regular reinforced concrete moment-resisting frames (RC-MRFs) with hysteretic energy dissipation devices (HEDD) mounted on chevron steel bracing. The main purpose of the if described study was to assess global seismic design parameters that could be easily inserted in the seismic design philosophy of Mexican codes. Different elastic stiffness ratios between the moment frame system and the whole structure (α) and between the hysteretic device and the supporting braces (β) were considered, among other relevant structural parameters, as described in following sections.

Fig. 1. 24-Story, reinforced concrete intermediate moment-resisting frame (RC-IMRF) building currently under construction in Mexico City.

2. RC-MRFS with HEDD under study

Perhaps the structural system most widely used in urban buildings in Mexico is RC-MRFs. Although Mexican RC codes do have provisions for ductile systems (special moment-resisting frames, SMRFs) since 1987, Mexican practicing engineers still prefer to design and build intermediate moment-resisting frames (IMRFs) according to the code (Fig. 1), but voluntarily applying some of the detailing requirements for SMRFs available in the code, particularly those related to the minimum confinement for beams and columns in the plastic hinge area (minimum spacing for required stirrups of 10 cm) and those related to bar splices, separation, etc. [26]. In addition, there is a large inventory of existing buildings in Mexico and many other nations which structural system is composed of non-ductile RC-MRFs. These facts pose a higher risk on RC-MRFs in regions worldwide where the seismic hazard is high. Therefore, because of all these reasons, the authors decided to study first the use of HEDD as structural fuses in RC-IMRFs buildings.

Hysteretic energy dissipation devices were mounted into RC-IMRFs using chevron bracing. The following design hypothesis were done: (a) RC-IMRFs were designed to carry gravitational loads plus their share of seismic lateral loads and respond essentially in the elastic range, (b) the supporting chevron system should remain essentially elastic under seismic loading also and, (c) HEDD are designed under seismic loading to behave inelastically up their maximum local displacement ductility capacity μ. Therefore, the structural system under lateral loading is composed by the RC-IMRFs and the chevron-bracing-HEDD system (Fig. 2). RC-IMRFs should be able to carry the gravitational loads after a strong earthquake (remaining essentially elastic), whereas HEDD should respond in the inelastic range of response as structural fuses and the supporting chevron bracing should remain essentially elastic.

For the parametric study, it was considered a series of buildings from 5 to 25 stories which typical plan layout is depicted in Fig. 3a. Perimeter frames are those where HEDD are mounted on chevron bracing as schematically depicted in Fig. 3b. Concurrent bracing at the building corners were studied because: (a) this configuration is often used in buildings in Mexico City and worldwide (Fig. 4), because for architectural reasons, central bays of perimeter frames are commonly used for the access of buildings and, (b) since it is not possible to study all relevant bracing configurations, from a seismic design viewpoint this configuration constitutes the worst-case design scenario for such systems, since this disposition exasperate the unfavorable concentration of axial loads in the columns. Therefore, if the proposed design procedure would be capable of reducing the axialization problem of corner columns to reasonable bounds, then it should be even more effective in more favorable bracing configurations.

It is also worth noting that, for simplicity, in this parametric study the location of elevators/stairs were not considered (Fig. 3a), because elevatoŕs cores are solved in many different ways depending on building configurations, heights and structural systems. For example, the following solutions are used in elevatoŕs cores: (a) frames with non-structural walls, (b) frames with infill walls, (c) structural shear walls (mostly RC walls) and, (d) braced frames. For medium-rise RC moment frame buildings (15 stories or higher), RC shear walls or braced frames are often used in elevatoŕs cores, which add lateral strength and stiffness but reduce the deformation capacity of such buildings. However, it is worth noting that the safe seismic design of medium-rise RC moment frames for Mexico Citý's soft soils do not depend on the presence of shear walls, as it has been demonstrated before for similar RC moment

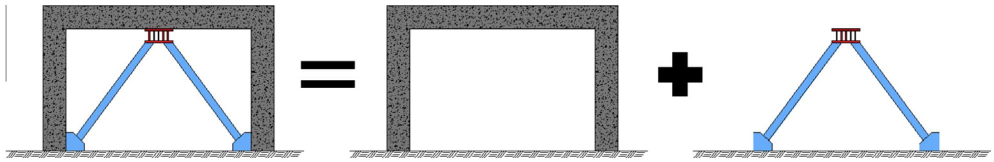

Fig. 2. Idealized system under lateral loading.

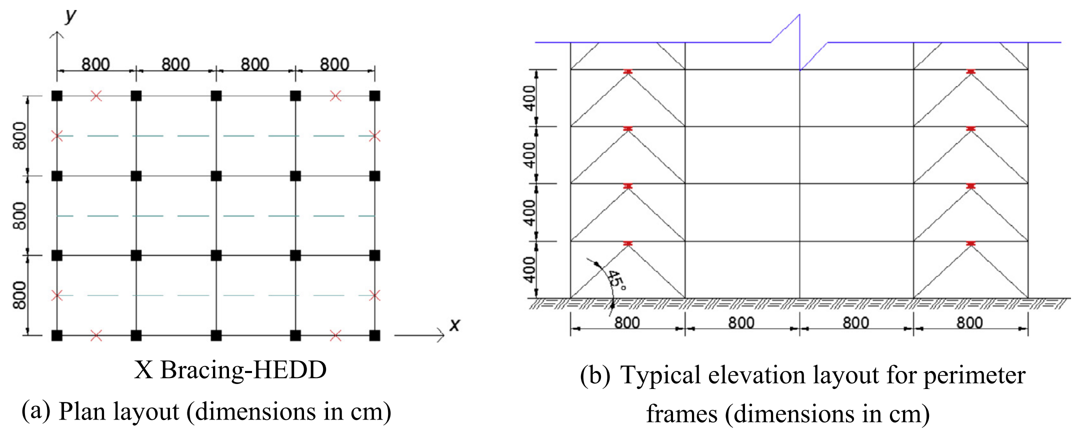

Fig. 3. Typical configuration for the buildings under study.

Fig. 4. Concentric braced framed buildings in Mexico City with concurrent chevron bracing at building corners.

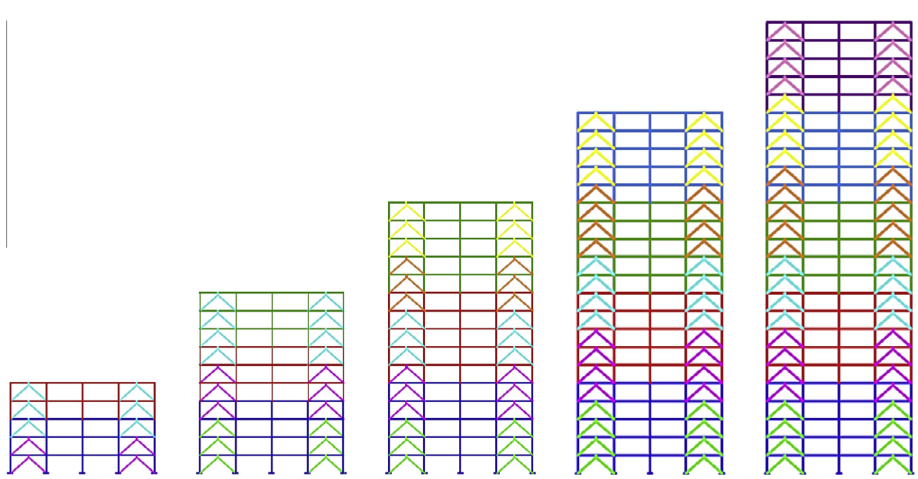

Fig. 5. Schematic display of the changes of cross sections for columns, beams and braces for the frames of the buildings under study.

Table 1
Typification of cross sections of main structural elements.

Number of stories for the models	Typification of cross sections on the identified story range		Number of stories for the models	Typification of cross sections on the identified story range	
	Columns and beams	Braces and HEDDs		Columns and beams	Braces and HEDDs
5	1–3	1–2	20	1–5	1–4
	4–5	3–5		6–10	5–8
10	1–4	1–3		11–15	9–12
	5–7	4–6		16–20	13–16
	8–10	7–10			17–20
15	1–5	1–3	25	1–5	1–4
	6–10	4–6		6–10	5–8
	11–15	7–9		11–15	9–12
		10–12		16–20	13–17
		13–15		21–25	18–21
					22–25

framed buildings up to 15 stories in height [26] or RC chevron braced framed buildings up to 24 stories in height [27].

The floor system was designed as a one-way ribbed RC slab (Fig. 3a). A geometric variable that was studied was the inclination of the chevron bracing with respect to a horizontal plane (θ), as a previous parametric study [28] suggested that the efficiency of HEDD on chevron devices depend on this parameter. Two angles were considered, $\theta = 40°$ (story height h = 336 cm) and $\theta = 45°$ (h = 400 cm), taking into account typical story heights for regular buildings in Mexico.

Therefore, building models had 5, 10, 15, 20 and 25 stories. Cross sections of beams, columns and braces were varied along the height (that is, different sections were used for beams, columns, braces and HEDDs through the height of the studied frames) as schematically depicted with different colors in Fig. 5 as identified in Table 1. It is worth noting that colors used in Fig. 5 are independent for each frame height, this is, they are not related from one frame height to another. For example, in the 5-story frames it is illustrated that brace sections are the same in stories 1 and 2 (magenta[1]) and from stories 3 to 5 (cyan), whereas columns of beams have the same cross sections from stories 1 to 3 (blue) and stories 4 to 5 (red). Then, this does not mean that "blue columns" of the 5-story models have the same cross sections that "blue columns" of the 10-story models, for example.

As a consequence of this design strategy, higher sections were used at the lower levels and relatively smaller sections were used at the top levels due to variation of story shears. It can be noticed also in Fig. 5 that, in order to minimize the potential formation of intermediate soft stories (stiffness and/or strength), columns and beams change sections in different stories than the chevron bracing. The designed cross sections are reported in detail in Nangullasmú [29].

3. Stiffness parameters under study

Three structural stiffness parameters were studied in order to evaluate their range of application under the general design assumptions already mentioned.

The first parameter is α, defined as the ratio between the elastic lateral stiffness for the frame (K_{frame}) with respect to the lateral stiffness of the whole frame-bracing-HEDD system (K_{total}):

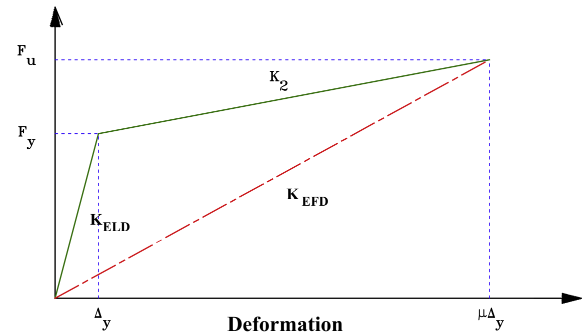

Fig. 6. Typical bilinear curve for an hysteretic energy dissipation device.

$$\alpha = \frac{K_{frame}}{K_{total}} \quad (1)$$

Three values of α were selected: $\alpha = 0.25$, where the RC-IMRFs are more flexible than the bracing-HEDD system, $\alpha = 0.50$, where the RC-IMRFs and the bracing-HEDD system have the same elastic lateral stiffness and $\alpha = 0.75$, where the RC-IMRFs are stiffer than the bracing-HEDD system.

The second parameter is β, the ratio between the elastic stiffness for the HEDD (K_{ELD}, Fig. 6) with respect to the elastic lateral stiffness of the supporting chevron braces (K_{diag}):

$$\beta = \frac{K_{ELD}}{K_{diag}} \quad (2)$$

Four values of β were chosen: $\beta = 1.0$, $\beta = 0.75$, $\beta = 0.50$ and $\beta = 0.25$. When $\beta = 1.0$ the stiffness of the bracing and the HEDD is the same (typical of BRBs). When $\beta < 1.0$, the HEDD is more flexible than the bracing supporting system, a desirable condition for most HEDD mounted in chevron bracing such as ADAS or TADAS devices. It is worth mentioning that some old RC buildings with IMRFs retrofitted in Mexico City with ADAS devices mounted on chevron bracing used the following range $0.25 \leqslant \beta \leqslant 0.50$ [30].

Finally, post to pre yielding stiffness ratios for the HEDD ($K_2/K_1 = K_2/K_{ELD}$, Fig. 5) of 0.0 (elastic–perfectly plastic), 0.03 and 0.05 were considered. Many researchers and practicing engineers often idealize HEDD as bilinear, elastic–perfectly-plastic. Nevertheless, it can be observed from experimental studies available in the literature that most HEDD develop a secondary stiffness different from zero [12,31,32]. Important differences in peak structural responses may be obtained considering a secondary stiffness different from zero with respect to an elastic–perfectly-plastic idealization for the HEDD for large ductility demands, as suggested in a previous parametric study [28].

A schematic tree diagram is depicted in Fig. 7 to summarize the described parametric study which it is reported in detail in Nangullasmú [29]. It can be deducted from Fig. 7 that for each height and θ angle there are 36 different models or combinations of parameters α, β, and K_2/K_{ELD}; therefore, there are 180 different models for each θ angle. Then, 360 different models were rigorously designed according to code guidelines and analyzed to perform this parametric study.

4. General design procedure

All models were designed using a procedure based upon the initial lateral elastic stiffnesses of the resisting elements. For the parametric study, a design base shear V of 10% of the total weight (W) for each structure was used ($V/W = 0.10$). The target (objective) maximum local displacement ductility (μ) for all hysteretic energy dissipation was assumed to be 10 ($\mu = 10$), independently of their location along the building height.

[1] For interpretation of color in Fig. 5, the reader is referred to the web version of this article.

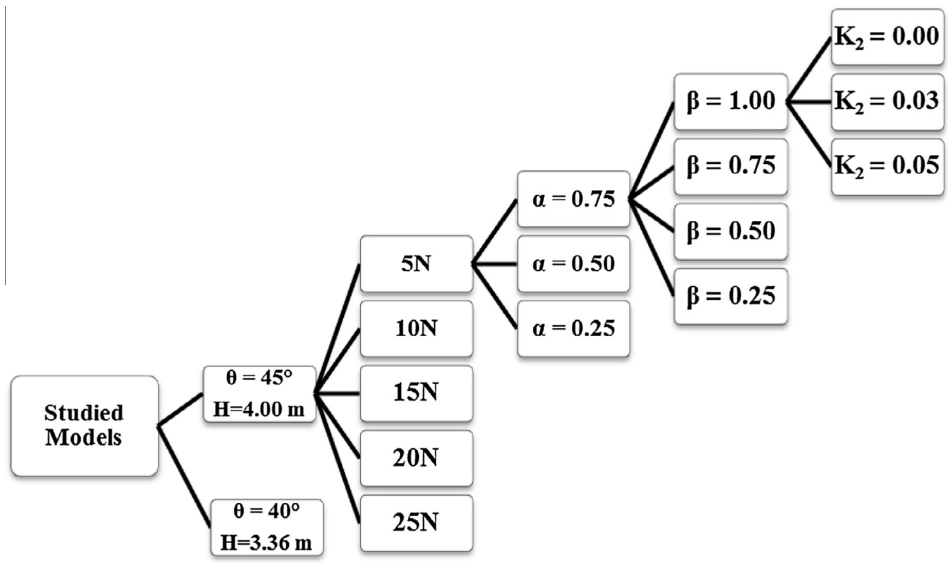

Fig. 7. Schematic tree diagram to identify the models studied by Nangullasmú [28].

The design procedure is reported in detail elsewhere [29,33], but it can be summarized as follows:

1. Define the design base shear. For this parametric study it was defined as $V/W = 0.10$, but for a code-oriented design procedure, it should be obtained using the procedures outlined by the code (this is, from the design spectrum).
2. Define the elastic lateral stiffness balance α that the moment frame is going to take (in this study $\alpha = 0.25$, $\alpha = 0.5$ and $\alpha = 0.75$), and from there obtain the lateral stiffness that the bracing-hysteretic device system should provide:

$$K_{frame} = \alpha K_{total} \tag{3}$$

$$K_{bracing\text{-}dissipator} = (1 - \alpha) K_{total} \tag{4}$$

It is worth noting that it is convenient to try to keep constant this α balance over the entire building height, provided that small variations would occur when selecting final design sections and typifying cross sections.

3. Define the design base shear that the moment frame should resist behaving essentially elastic in absence of the bracing-hysteretic device system:

$$V_{frame} = \alpha V \tag{5}$$

using this base shear and the static method, equivalent lateral seismic forces can be defined.

4. Develop an analytical model for the moment frame for the preliminary design of beams and columns in absence of the bracing-hysteretic device system, using the obtained lateral loads and including the vertical loads. The frame must comply with serviceability state limits under vertical loads, but not yet for lateral loads.
5. Once the frame sections have been pre-designed, the lateral stiffness for the moment frame (K_{frame}) could be assessed using any recognized method already available in the literature. For simplicity, in this work Wilbuŕs formula was selected. Assuming that all stories have the same height h and all beams have the same length l, for the first story under a fixed-based condition:

$$K_{frame} = \frac{24E}{h^3\left(\frac{2}{\sum_{i=1}^{ncol} I_{ci}} + \frac{1}{\frac{h}{l}\sum_{j=1}^{nbeam} I_{bj} + \frac{1}{12}\sum_{i=1}^{ncol} I_{ci}}\right)} \tag{6}$$

where E is Young's modulus for the frame elements, I_{ci}, I_{bj}, $ncol$ and $nbeam$ are respectively the moments of inertia of column i, the moment of inertia of beam j, the number of columns and the number of beams in the first story respectively. For an intermediate story of interest k, under similar assumptions, Wilbuŕs formula can be reduced as:

$$K_{frame} = \frac{24E}{h^3\left(\frac{2}{\sum_{i=1}^{ncol} I_{ci}} + \frac{1}{\frac{h}{l}\sum_{j=1}^{nbeam} I_{bj_{k-1}}} + \frac{1}{\frac{h}{l}\sum_{j=1}^{nbeam} I_{bjk}}\right)} \tag{7}$$

6. The horizontal and vertical distribution of the proposed braced-energy dissipation system should be as uniform as possible. From Eq. (5) it should be determined the lateral stiffness and strength for the bracing-hysteretic device system for preliminary design purposes, then:

$$K_{bracing\text{-}dissipator} = (1 - \alpha) K_{total} = n K_{eq} \tag{8}$$

where n is the number of braces required to mount the hysteretic energy dissipation devices, K_{eq} is the stiffness of an equivalent axial element that takes into account the elastic stiffness for the bracing ($K_{bracing}$) and the effective stiffness of the hysteretic energy dissipation device at the objective maximum local displacement ductility μ, K_{EFD} (Fig. 6). For symmetric chevron bracing with an angle of inclination θ with respect to a horizontal plane:

$$\frac{1}{K_{eq}} = \frac{1}{K_{bracing}} + \frac{2\cos^2\theta}{K_{EFD}} \tag{9}$$

where

$$K_{bracing} = \frac{E_{bracing} A_{bracing}}{L_{bracing}} \cos^2\theta \tag{10}$$

$$K_{EFD} = \frac{K_{ELD} + K_2(\mu - 1)}{\mu} \tag{11}$$

where K_{EFD}, K_{ELD}, K_2 and μ are completely defined in Fig. 6 (bilinear model). In this study, three different values were chosen for K_2: $K_2 = 0$, $K_2 = 0.03K_{ELD}$ y $K_2 = 0.05K_{ELD}$. It can be demonstrated that from Eqs. (2), (9) and (11) that:

$$K_{eq} = \frac{\beta K_{bracing} + K_2(\mu - 1)}{\beta + 2\mu\cos^2\theta + \frac{K_2(\mu-1)}{K_{bracing}}} \tag{12}$$

A decision should be made about the objective values for μ and β. As explained before, in this parametric study it was assumed that $\mu = 10$ for all HEDD and $\beta = 1.0$, $\beta = 0.75$, $\beta = 0.5$ and $\beta = 0.25$. Based upon these assumptions, the required elastic stiffnesses for the bracing and the hysteretic dissipaters were assessed.

On the other hand, the bracing-hysteretic energy dissipation system should provide the following lateral strength at the first yielding of the energy dissipator:

$$V_{bracing\text{-}dissipator} = (1 - \alpha)V = nV_{u_{B-D}} \tag{13}$$

where $V_{u_{B-D}}$ is the shear strength that each equivalent axial element representing the bracing-hysteretic energy dissipation device system should supply. This shear strength depends on the maximum force F_u of the energy dissipation device at the objective displacement ductility μ (Fig. 6). Therefore, under a chevron bracing mounting, it can be determined that for each hysteretic passive energy dissipation device:

$$F_u = 2V_{u_{B-D}} \tag{14}$$

From the primary bilinear curve (Fig. 6), F_u can also be assessed as:

$$F_u = K_{EFD}\mu\Delta_y \tag{15}$$

Therefore, once F_u has been determined, the yield displacement for each hysteretic energy dissipation device can be calculated as:

$$\Delta_y = \frac{F_u}{\mu K_{EFD}} \tag{16}$$

With this information, one can define the dimensions of any hysteretic energy dissipation device using expressions already available in the literature [1,12,16–18,31,32,34]. However, it is worth noting that, for this general parametric study, theoretical balances were used, as it was not the purpose of this study to evaluate a particular hysteretic passive energy dissipation device.

It also worth noting that for the design of the braces is not only important to assess the required stiffness (Eq. (10)), but to warrant that they will remain elastic when the hysteretic energy dissipation devices would develop their maximum displacement ductility μ. Therefore, the maximum axial load that each brace would carry is:

$$P_{bracing} \geq \frac{F_u}{2\cos\theta} \tag{17}$$

Then, since axial compression often controls the design of bracing, then the bracing should be designed to have a reasonable safety factor for buckling. In this study a minimum factor of safety of 1.5 was used, as described in detail in Nangullasmú [29]. Therefore, the bracing design is performed by satisfying simultaneously Eqs. (10) and (17), and this may require an iterative procedure.

7. Once the preliminary design for all members has been done, an *ad-hoc* elastic analytical model for the whole building is built, using the equivalent secant stiffness K_{EFD} at the objective ductility μ for the hysteretic energy dissipator (Eq. (11), Fig. 6), that should be analyzed again under vertical loads and the lateral load distribution corresponding to the design base-shear ($V/W = 0.10$ in our study). All elements should be revised for strength and deformation again in the described sequence below.
8. *Hysteretic energy dissipators:* As in this parametric study it was assumed that all HEDD ideally are capable of taking their load share while developing the target ductility $\mu = 10$ and no specific HEDDs are being designed (for example ADAS, TADAS, BRBs, etc.) then, this was fulfilled without any iteration. However, for a given HEDD of interest, dimensions are defined in terms of their required lateral stiffness and yield strength. For example, in ADAS elements one should proposed the height, the plate thickness and the required number of plates, knowing μ, F_u, Δ_y and K_{EFD}.
9. *Steel braces:* Once there is a preliminary design for the HEDD, steel braces should be reviewed to carry the axial loads obtained from the refined analysis while satisfying the minimum factor of safety for buckling of 1.5. In case that the braces do not satisfy this requirement, one should propose newer brace sections that would satisfy this requirement and return to step 7. If the requirement is satisfied, then continue.
10. *RC beams:* Using the bending moments and shear forces from the analysis considering all required load combinations, RC beams are designed according to the reinforced concrete code guidelines of interest (for example, NTCC-2004 [35] or ACI-318 [36] codes) for IMRFs. In case that beams do not fulfill all requirements, one should proposed newer beam sections and then return to step 7. Otherwise, the design procedure should continue.
11. *RC columns:* They should be designed for combined bending, axial loads and shear forces from the analysis considering all required load combinations according to the reinforced concrete code guidelines of interest for IMRFs. It is worth noting that in order to define the critical axial load for design, the following criteria was used: (a) axial loads from analyses and, (b) the axial load that the column should carry for gravitational loads only plus the maximum axial load transmitted by the braces above if all of them would be able to develop their nominal buckling load. In order to review the strong column weak-beam, it should be checked that at the joint, $\Sigma M_c \geqslant \eta\Sigma M_g$, where ΣM_c and ΣM_g are respectively the sum of the unfactored nominal design moments for columns and beams at the joint, where $\eta = 1.5$ for NTCC-2004 [35] (ACI-318 [36] specifies $\eta = 1.2$). In the event that some columns do not fulfill all requirements, one should proposed newer column sections that would satisfy all requirement and then return to step 7. If requirements are satisfied, then continue.
12. *Connections:* Beam-column-brace joints should fulfill code requirements for IMRFs and IMRBFs. If they do not satisfy a requirement, newer sections (columns and/or beams usually) should be proposed and then return to step 7. Otherwise, the design procedure should continue.
13. As strength and detailing requirements are already satisfied, it should be reviewed that the final stiffness balances (α and β) would be close to initial assumptions over the building height, particularly if many cross sections were modified in the design process (steps 8–12). These could be done in several ways using the final analytical model, or using Wilbur's formula.
14. The whole structure should also be revised to satisfy with lateral deformations limit states according to code guidelines or other performance objectives. In this parametric study no limits were defined, as one of the purposes of this research is to assess how these limits should be in order to obtain a suitable mechanism according to the fuse design concept. However, for a fully code-designed structure, if the final designed building does not satisfy limit states for lateral deformations, it would mean that the building is more flexible than what the code is allowing. Therefore, a stiffer structure needs to be designed. A practical solution is to increase the stiffness of the bracing-HEDD system; this is, to propose a smaller α parameter. There are some possibilities to achieve this goal: (a) reduce the target ductility demand for the HEDD (in this case, propose $\mu < 10$), (b)

increase the elastic stiffness for the HEDD (increase β) or, (c) increase the cross sections for the braces (increase $K_{bracing}$). After taking a decision on this regard, one should return again to step 7. If step 14 is fulfilled, the design procedure is over.

5. Nonlinear static analyses

Nonlinear static analyses (pushover) were conducted for each model under study. All elements (columns, beams, braces and HEDDs) were modeled to monitor the possibility of developing a nonlinear behavior, as described in detail elsewhere [29]. The nonlinear bilinear behavior of the HEDDs was modeled by equivalent beam-column elements connected to the chevron braces and beams, according to a previously validated procedure which is outlined in detail elsewhere [34]. P–Δ effects were considered in the analyses. For simplicity, lateral load distribution profiles based upon the first mode of vibration were used in the pushover analysis. This was done to have a general framework of comparison, taken into account that: (a) building height ranges from 5 to 25 stories, (b) the modal mass associated to the fundamental mode is higher than 60% for most buildings and, (c) for similar buildings, it was demonstrated [37,38] that modal pushover analysis is not a suitable method to determine average global design parameters for the structural system of interest. In addition, for this system and for the purpose of assessing global design parameters only, higher mode effects were found to have a reduced impact in assessing peak lateral drifts even for the upper stories, where larger differences are expected when comparing the results obtained with pushover analyses based upon the fundamental mode with those obtained with modal pushover analyses as presented in the literature [39,40]. Of course, higher mode effects are very important in the nonlinear dynamic response of multi-story and very tall buildings, something which it is out of the scope of the present study.

The main results obtained from nonlinear static analyses were: (a) normalized story and global lateral shear vs drift curves (V/W vs Δ) and, (b) yielding mapping corresponding to the load step where the collapse mechanism was formed. From the story and global shear vs drift curves the following information was obtained: (a) Overstrength factors (Ω), (b) ductility reduction factors (Q), (c) apparent peak story and global ductility capacities, (d) equivalent story drift at yielding (Δ_y), (e) peak story drifts (Δ_{max}). The obtained results for the 360 models are reported and discussed in greater detail in Nangullasmú [29].

6. Mappings of the intensity of inelastic responses

A hot color scale was defined to highlight the inelastic demands of all structural elements (i.e., Table 2 and Fig. 8). No color identifies an elastic response. A yellow color identifies nonlinear response after yielding and up to a reparable damage state for conventional structural elements ($\phi/\phi_u \leqslant 0.25$), and for HEDDs $1 < \mu < 6$. Orange is used for moderate nonlinear responses for conventional structural elements ($0.25 < \phi/\phi_u \leqslant 0.5$) and for HEDD $6 < \mu < 8$. Red is used for important nonlinear responses for conventional structural elements (up to peak response, $0.5 < \phi/\phi_u \leqslant 0.75$) and for HEDD $8 < \mu < 10$. Brown is used for nonlinear response on the descending branch of moment–curvature curves for conventional structural elements ($0.75 < \phi/\phi_u \leqslant 1.0$) and for HEDD $10 < \mu < 12$. Although the inelastic behavior of braces was considered in all studied models, all braces for all studied models remained elastic during the performed pushover analyses, so there was no need to identify a color scale for inelastic axial extensions or bucking shortenings.

Table 2
Color intensity scale used for the HEDD.

Color	Ductility demand
(brown)	$10 < \mu \leqslant 12$
(red)	$8 < \mu \leqslant 10$
(orange)	$6 < \mu \leqslant 8$
(yellow)	$2 < \mu \leqslant 6$
	Elastic

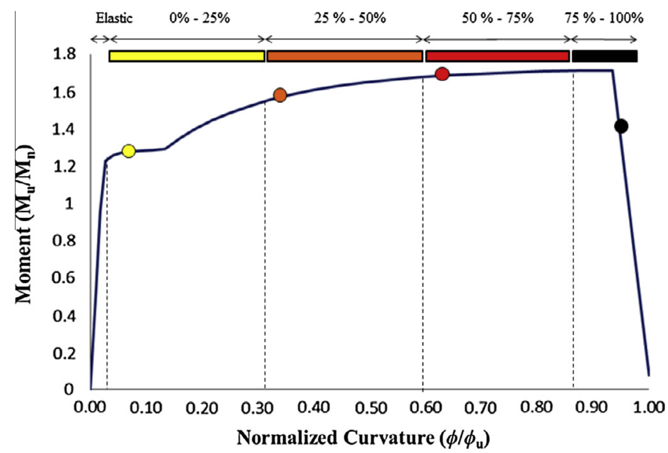

Fig. 8. Schematic color intensity scale for the inelastic responses of the assessed moment-normalized curvature curves for beams and columns.

To help illustrate the impact of the postyielding stiffness K_2, the final yielding mappings for the 10-story models where $\theta = 45°$, $\alpha = 0.25$ and $\beta = 0.25$ are depicted in Fig. 9. It can be observed that as K_2 increases, the inelastic action also increases, in terms of the hot colors scale. In fact, the plastic rotations in the left perimeter columns increases, as a consequence that higher axial forces are transmitted by the braces. Although the yielding sequence suggests that the desired collapse mechanism can be formed, the major problem is that if high displacement ductility demands (μ) are allowed for the HEDD, important plastic rotations could be developed in the perimeter columns if the bilinear behavior observed in the HEDD in experiments is taken into account, then leading to an undesirable condition.

To help illustrate the impact on β, the ratio between the elastic stiffness for the HEDD with respect to the elastic lateral stiffness of the supporting chevron braces (K_{diag}), the final yielding mappings for the 5-story models where $\theta = 45°$, $\alpha = 0.25$ and $K_2 = 0.05K_{ELD}$ are depicted in Fig. 10. A general tendency observed in most of the studied models is illustrated in this figure, where the inelastic response of the HEDD (in terms of μ) increases as β decreases, this is, HEDDs tend to become more efficient a β decreases. However, for large μ values, the members of the frame (beams and columns) also experience important inelastic rotations, particularly in models with ten or more stories.

The impact of α, the ratio between the elastic lateral stiffness for the frame (K_{frame}) with respect to the lateral stiffness of the whole frame-bracing-HEDD system (K_{total}) is that as α increases, the inelastic response of the moment frame increases and therefore, damage is concentrated more in beams and columns (not shown).

In following sections it will be shown and discussed only the models which inelastic action is closer to the initial design assumptions for each height under study, this is, those frame models where the HEDD mostly concentrate the inelastic deformations by developing high ductility demands whereas the yielding of beams and columns is much smaller, particularly in columns.

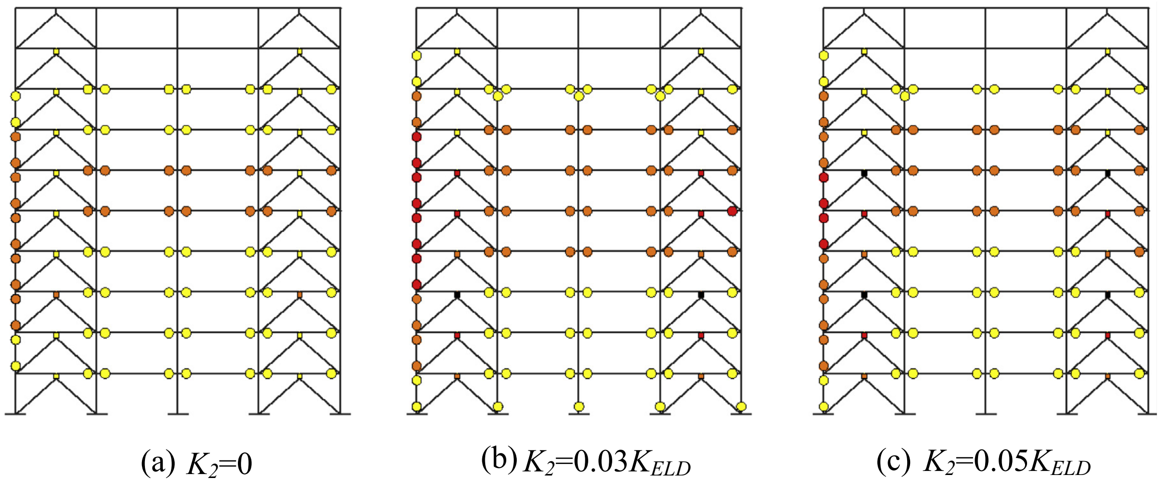

Fig. 9. Inelastic demands mapping for 10-story models where $\theta = 45°$, $\alpha = 0.25$ and $\beta = 0.25$.

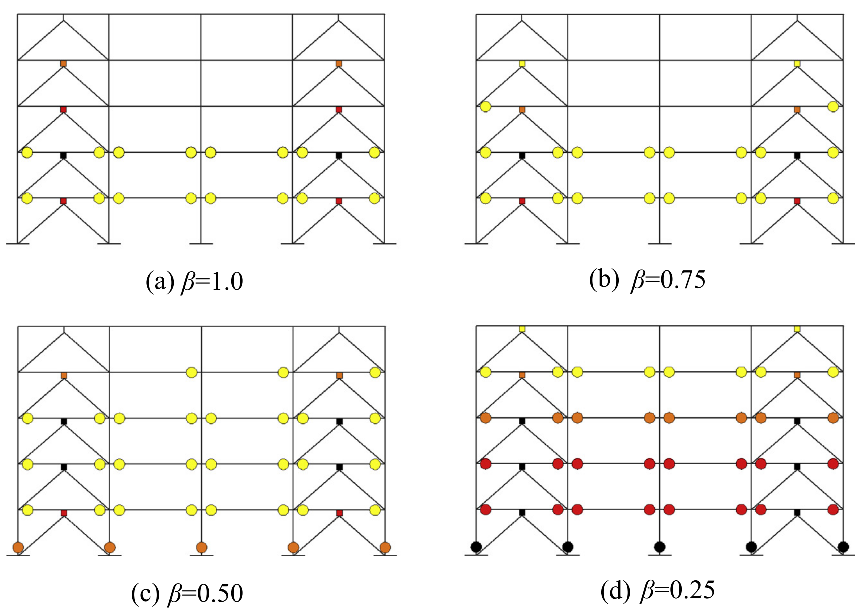

Fig. 10. Inelastic demands mapping for 5-story models where $\theta = 45°$, $\alpha = 0.25$ and $K_2 = 0.05K_{ELD}$.

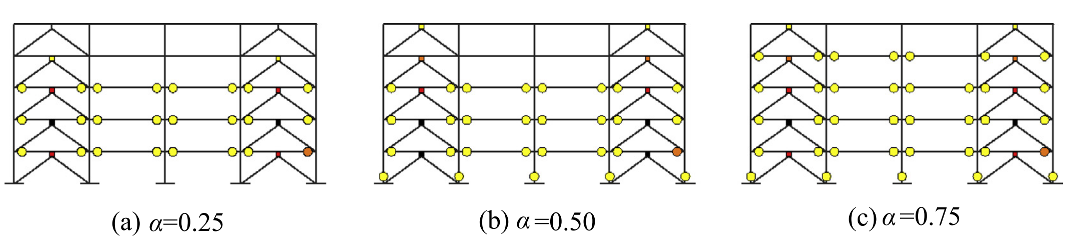

Fig. 11. Inelastic demands mapping for 5-story models where $\theta = 40°$, $\beta = 0.25$ and $K_2 = 0.05K_{DDE}$.

6.1. Lowrise models (5-story models)

The final yielding mappings for the 5-story models where $\beta = 0.25$ and $K_2 = 0.05K_{ELD}$ for different values of α are depicted in Figs. 11 and 12 when $\theta = 40°$ and $\theta = 45°$ respectively. It can be observed (taking into account the described color scales) that most of the inelastic action is concentrated in the HEDD, where important ductility demands are developed. For the frame elements, incipient yielding is mostly observed at beams ends. Yielding of the first story columns at their base are developed as a consequence of the fixed-base assumption. From the viewpoint that a suitable mechanism in a structure with HEDD is achieved when the hysteretic devices yield first and develop their maximum local displacement ductility μ, whereas in the moment frame incipient yielding (if any) is only formed at the beam ends, the closest result is obtained when $\alpha = 0.25$, $\beta = 0.25$, $\theta = 40°$ and $K_2 = 0.05K_{ELD}$

(Fig. 11a). No important differences are observed in the yielding mechanisms for this story height with respect to the angle of inclination θ of the chevron braces (Figs. 11 and 12).

To complete the picture, the displacement ductility demands (μ) for the HEDDs of the models depicted in Figs. 11 and 12 are presented in Figs. 13 and 14 for the different K_2/K_{ELD} ratios under study. In these figures, the vertical dotted lines highlight the ductility range where the performance of the HEDDs could be considered efficient ($8 \leqslant \mu \leqslant 12$). It is observed from the results depicted in Figs. 13 and 14 that the post-yielding stiffness K_2 of the HEDDs is an important parameter for the global performance of the structure and the HEDDs themselves. In general, as K_2 increases, the ductility developed by the HEDDs also tends to increase. In fact, it is observed that for an elastic perfectly-plastic assumption ($K_2 = 0$), the HEDDs do not achieve the target ductilities for an efficient performance. As a matter of fact, as β decreases, the differences between elastic perfectly-plastic ($K_2 = 0$) and others ($K_2 \neq 0$) bilinear behaviors for the HEDDs increases (not shown, Nangullasmú [29]). However, a similar behavior is observed for the bilinear models under study ($K_2 = 0.03K_{ELD}$ and $K_2 = 0.05K_{ELD}$), this is, no important differences are observed.

Why the ductility demands increases for the HEDD as K_2 increases? The reason is that since K_2 is being directly taken in the design procedure (Eq. (11), Fig. 6), although elastic–perfectly plastic ($K_2 = 0$) and the other bilinear isolators ($K_2 \neq 0$) are designed to provide the same ultimate maximum force F_u (Eq. (15), Fig. 6), it can be observed from Fig 6 that the yielding force F_y for the other bilinear isolators ($K_2 \neq 0$) is smaller than for the elastic–perfectly plastic isolators ($K_2 = 0$), so bilinear isolators with $K_2 \neq 0$ ended working first in the inelastic range than elastic–perfectly-plastic isolators.

It is not uncommon to find out in the literature recommendations based upon the assessment (maximization, minimization) for a single design parameter without looking at the same time to other parameters or the overall performance for the structure. It is worth noting that this practice does not warrant taking good design decisions. For example, from an "efficient" design viewpoint, it is tempting to design for the largest ductility demands

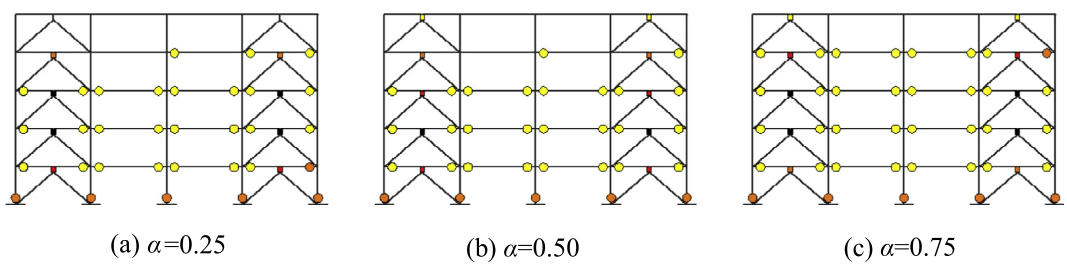

Fig. 12. Inelastic demands mapping for 5-story models where $\theta = 45°$, $\beta = 0.25$ and $K_2 = 0.05K_{DDE}$.

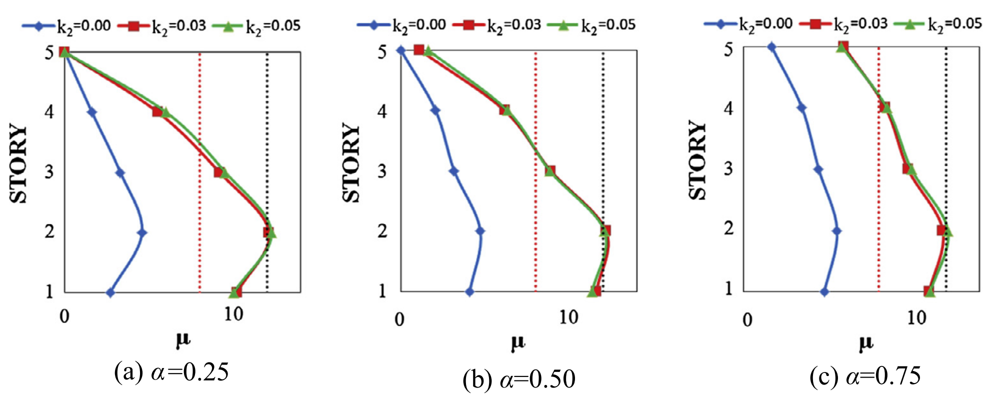

Fig. 13. Ductility demands (μ) for the HEDD for 5-story models where $\theta = 40°$ and $\beta = 0.25$.

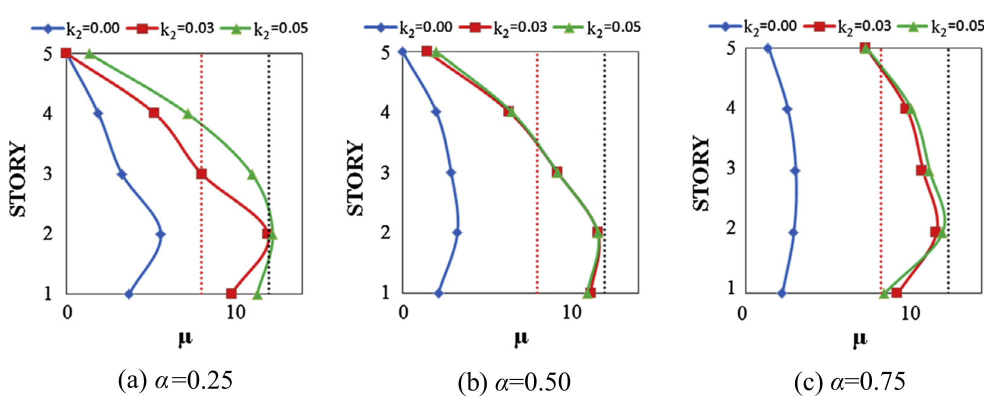

Fig. 14. Ductility demands (μ) for the HEDD for 5-story models where $\theta = 45°$ and $\beta = 0.25$.

(μ) in most HEDDs in most stories, if possible. Therefore, looking only at the information depicted in Figs. 13 and 14, one may conclude that the best combination of structural parameters are obtained when $\alpha = 0.75$, $\beta = 0.25$ and $K_2 = 0.05K_{ELD}$ (Figs. 13c and 14c). However, it is also observed in Figs. 11 and 12 that for such combination of parameters, the inelastic response of beams and columns increases (Figs. 11c and 12c) with respect to other values of α that lead to a more reduced inelastic behavior for beams and columns (for example, $\alpha = 0.25$, Figs. 11a and 12a). Perhaps the inelastic yielding developed mostly in beams for the models where $\alpha = 0.75$ (Figs. 11c and 12c) is still acceptable for the 5-story models. However, for taller models, allowing such high ductility demands for the bilinear HEDDs may lead to important yielding in some columns, that it is not acceptable, as it is briefly illustrated in following sections and in detail in Nangullasmú [29].

6.2. Medium-rise models (10-story and 15-story models)

In general, some differences are observed in the inelastic demand mappings for the 10 and 15 story models when θ varies from 40° to 45°. The models with closer correlation with the original design assumptions are depicted in Fig. 15. The inelastic

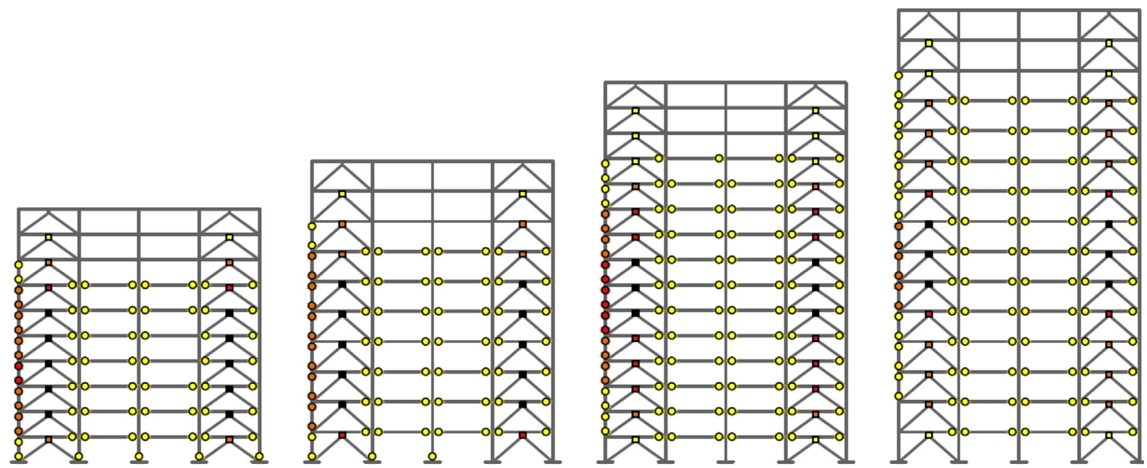

(a) α=0.25, β=0.75, θ=40° (b) α=0.25, β=0.50, θ=45° (c) α=0.25, β=0.75, θ=40° (d) α=0.25, β=0.50, θ=45°

Fig. 15. Inelastic demands mapping for 10-story and 15-story models when $K_2 = 0.05K_{DDE}$.

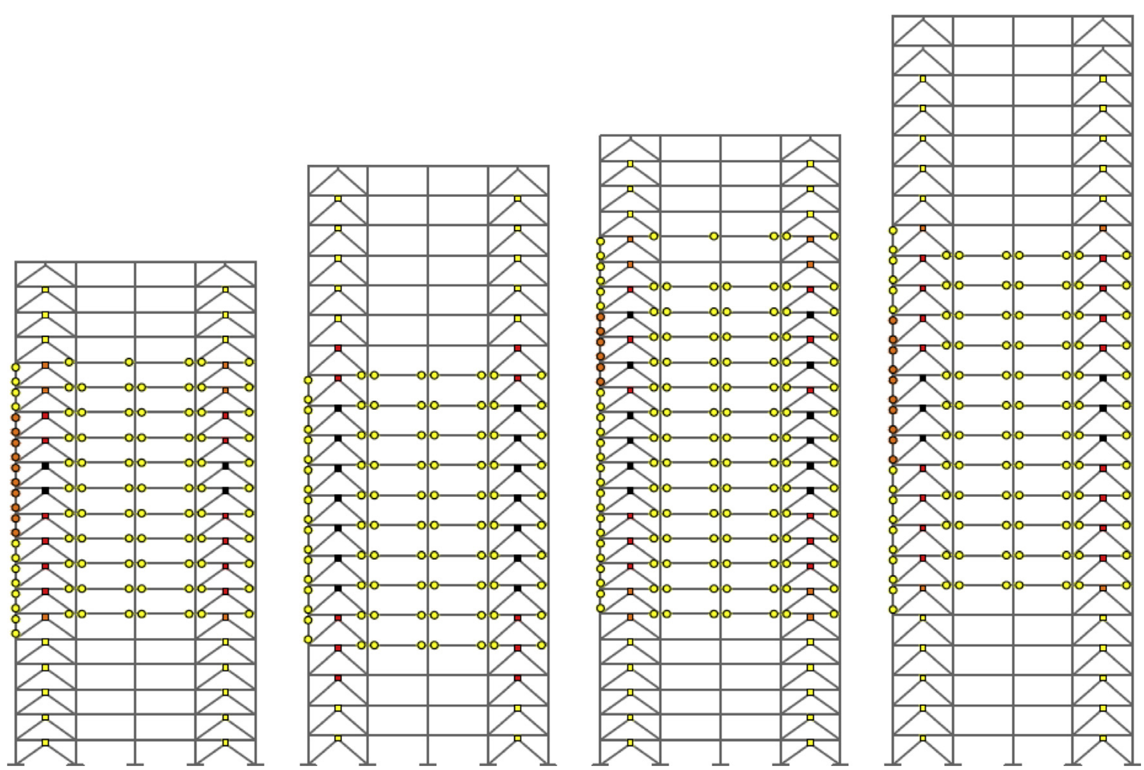

(a) α=0.50, β=0.50, θ=40° (b) α=0.50, β=0.75, θ=45° (c) α=0.50, β=0.50, θ=40° (d) α=0.50, β=0.75, θ=45°

Fig. 16. Inelastic demands mapping for 20-story and 25-story models when $K_2 = 0.05K_{DDE}$.

demand mappings when $\theta = 40°$, $\alpha = 0.25$ and $\beta = 0.75$ are shown in Fig. 15a and c for the 10-story and the 15-story models respectively. In such figures it can be observed that more than 60% of the HEDDs develop reasonably large ductility demands (in agreement with the original design hypothesis), but the HEDDs at the top level do not yield. Most beams develop incipient yielding in reasonable bounds; however, left exterior columns experience important plastic rotations primarily at the intermediate levels, which it is not a satisfactory performance according to the original design assumptions. When $\theta = 45°$ (taller models), the closer performances with respect to the design assumptions are obtained when $\alpha = 0.25$ and $\beta = 0.50$, as shown in Fig. 15b and d for the 10-story and 15-story models respectively. For practical purposes, the inelastic demands mappings are similar with respect to those discussed when $\theta = 40°$ (Fig. 15a and c). However, the difference is that a smaller stiffness for the HEDDs is needed (smaller β), as β reduced from 0.75 to 0.5.

6.3. 20-story and 25-story models

Similarly to what it was observed for the 10-story and 15-story models, some small differences are observed in the inelastic demand mappings for the 20 and 25 story models when θ varies from 40° to 45°. The models with closer correlation with the original design assumptions are depicted in Fig. 16, and for $\theta = 40°$ are obtained when $\alpha = 0.50$ and $\beta = 0.50$ (Fig. 16a and c) for the 20-story and the 25-story models respectively, whereas for $\theta = 45°$ are obtained when $\alpha = 0.50$ and $\beta = 0.75$ (Fig. 16b and d). From these figures it is worth noting that the HEDDs only develop ductility demands according to the design assumptions primarily at the intermediate levels (about 60% of the HEDDs), as ductility demands at the bottom stories are relatively low and at the upper stories are also small or even elastic behaviors are obtained. Inelastic deformations in beams and columns are also concentrated primarily at the intermediate levels. The reason why the plastic hinges shifted away from the bottom stories is that relatively stronger frames (wider sections) at those stories were obtained as a consequence that the design α parameter increased from 0.25 to 0.50. Most beams developed a satisfactory performance with a reduced or incipient yielding. However, left exterior columns at the intermediate levels experienced important plastic rotations, which it is not desirable.

7. Assessment of global design parameters

Once all inelastic demand mappings and their relation with the ductility demand curves for the HEDDs (i.e., Figs. 13 and 14) for all the studied models were carefully analyzed, the information obtained from pushover analyses was used to carefully assess global design parameters, as briefly discussed in following sections.

7.1. Best stiffness ratios

Based upon the observation of the inelastic demand mappings and the ductility demand graphs for the HEDDs (i.e., Figs. 13 and 14), apparently "better" or "best" α and β stiffness ratios were defined, as summarized in Table 3.

It can be concluded that for the geometry and the stories under study, in order to obtain a design close to the structural fuse concept, it is desirable that the elastic stiffness of the HEDDs should be 50% or a bit more the elastic stiffness of the supporting braces, that is, $0.5 \leqslant \beta \leqslant 0.75$. These limited range value for β is a direct consequence of the non-ductile detailing (and behavior) for beams and columns, as for large μ values for the HEDDs, beam columns experience important inelastic rotations. That is why smaller values for β cannot be recommended, as μ increases as β decreases.

Table 3
Best α and β stiffness balances for the models under study.

STORIES	H/L	θ (°)	α	β
5	0.53	40	0.25	0.50
	0.63	45	0.25	0.50
10	1.05	40	0.25	0.75
	1.25	45	0.25	0.50
15	1.58	40	0.25	0.75
	1.88	45	0.25	0.50
20	2.10	40	0.50	0.50
	2.50	45	0.50	0.75
25	2.63	40	0.50	0.50
	3.13	45	0.50	0.75

With respect to the stiffness parameter α, it can be observed that for models up to 15 stories or models that are not very slender ($H/L < 2$), the most efficient system is obtained when the elastic lateral stiffness for the frame is 25% the lateral stiffness for the complete system ($\alpha = 0.25$), in other words, the bracing-HEDD system is stiffer than the frame alone. However, as frames become taller (20 and 25 stories) and/or their slenderness ratio increases ($H/L > 2$), it is required that the lateral stiffness for the frames increases with respect to the one for the bracing-HEDD system, this is, that α increases and, hence, stiffer frames and more flexible bracing-HEDD systems have to be designed. Again, the limited range value for α is also related to the non-ductile detailing for beams and columns.

7.2. Story drifts

Story drifts related to the first yielding (Δ_y) and to the limit state described before (Δ_u) for the complete system were assessed from idealized bilinear story shear vs story drift curves from pushover analyses (for example, Fig. 17) and they are reported in detail in Nangullasmú [29]. It was observed that Δ_u increases as: (a) the HEDDs are more flexible (β decreases) and, (b) the postyielding stiffness (K_2) of the HEDDs increases.

In order to define story drift for design purposes, Δ_y and Δ_u envelopes for the "best" stiffness ratios identified in Table 3 were

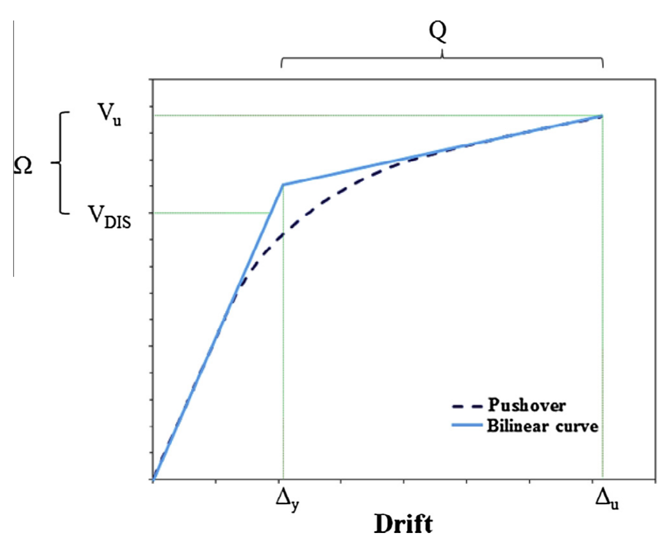

Fig. 17. Idealized bilinear shear vs drift curves (story and global) from pushover analyses. Global design parameters Q and Ω are assessed from the global base shear vs global drift curve.

assessed. The envelopes obtained for the best stiffness balances for the 5-story, 15-story and 25-story models when $\theta = 45°$ and $K_2 = 0.05K_{ELD}$ are depicted in Fig. 18. Peak drift values were obtained at the stories where the HEDDs developed their higher ductilities. It can be observed from Fig. 18 that for low and medium rise models (5–15 stories), Δ_u varied from 0.013 to 0.022 (1.3–2.2% drift); the highest Δ_u value was obtained for the 5-story model (Fig. 18a). Also, for the 5–15 story models, Δ_y varied from 0.002 to 0.004. For the taller and/or slender models (20 and 25 stories), Δ_u varied from 0.012 to 0.015 whereas Δ_y varied from 0.001 to 0.003. As it can be observed, it might not be wise enough to recommend an average value for Δ_u and Δ_y, as they also depend on the combination of the relative stiffness parameters α and β, and there is not a single combination that defines the best performance for the models under study.

7.3. Seismic response modification factor Q

In Mexican codes, Q is defined as the seismic response modification factor used in the design that accounts for the deformation capacity, so it can be obtained from the global base shear vs global drift idealized bilinear curve as $Q = \Delta_u/\Delta_y$ (Fig. 17). Under this definition, Q values were assessed for all models under study. An important effort was done to synthesize in a compact table format the best performances of the models under study, taking into account the desirable mechanism of strong column-weak beam – strong bracing-weakest HEDD (structural fuse). The results when $\theta = 40°$ and $\theta = 45°$ are reported in Tables 4 and 5, and one may have a clue of the range of application of the parameters under study. In Tables 4 and 5 color shades are used in parameters β, μ and Q to identify the following global behavior: (1) no color shade is used when there is no yielding in frame elements or there are few incipient yielding in beams, (2) yellow shades identify tolerable yielding in beams and incipient yielding (if any) on few columns and, (3) orange shades are used when inelastic rotations on beams are important, as well as important inelastic rotations are formed at both ends of columns at some intermediate levels, which may lead to local failures and/or soft story responses.

It can be observed from Tables 4 and 5 that the best performances are obtained when $0.5 \leqslant \beta \leqslant 1.0$. As stated earlier, as β decreases, the structural damage (inelastic demand) on beams and columns increases, as μ and Q increases. This is very important, as abusing on the ductility (μ) that HEDDs could develop may lead to undesirable structural performances. It is also worth noting that if one uses for design the Q value identified in Tables 4 and 5, which is associated to the largest ductility demands (μ) for the HEDD considered in this study, in several cases it will be tolerated incipient damage in beams and in some columns of the IMRFs at the intermediate levels, which is not 100% in agreement with the original design philosophy.

Table 4
Recommended values of the structural parameters when $\theta = 40°$.

Stories	α	K_2/K_{ELD}	β	μ	Q
5	0.25	0	0.50-1.0	6-10	3.7-4.6
		0.03	0.50-1.0	12-8	5.7-5.3
		0.05	0.50-1.0	12-8	5.6-5.2
10	0.25	0	0.50-1.0	8-6	4.9-4.2
		0.03	0.50-1.0	12-8	6.6-6.1
		0.05	0.50-1.0	12-8	6.8-6.3
15	0.25	0	0.50-1.0	<6	2.4-2.5
		0.03	0.50-1.0	12-8	6.0-5.6
		0.05	0.50-1.0	12-8	6.4-5.5
20	0.50	0	0.50-1.0	6-10	2.9-3.9
		0.03	0.50-1.0	12-8	4.4-3.8
		0.05	0.50-1.0	12-8	4.3-3.7
25	0.50	0	0.50-1.0	10-6	5.1-3.9
		0.03	0.50-1.0	12-8	5.3-4.6
		0.05	0.50-1.0	12-8	5.1-4.3

Table 5
Recommended values of the structural parameters when $\theta = 45°$.

Stories	α	K_2/K_{ELD}	β	μ	Q
5	0.25	0	0.50-1.0	6-10	3.7-4.3
		0.03	0.50-1.0	10-8	4.4-4.1
		0.05	0.50-1.0	10-8	5.1-4.5
10	0.25	0	0.50-1.0	8-6	3.5-4.0
		0.03	0.50-1.0	12-8	6.6-6.3
		0.05	0.50-1.0	12-8	6.1-5.8
15	0.25	0	0.50-1.0	<6	2.0-2.4
		0.03	0.50-1.0	12-8	5.6-5.5
		0.05	0.50-1.0	12-8	5.7-5.4
20	0.50	0	0.50-1.0	8-10	4.0-4.8
		0.03	0.50-1.0	12-8	4.8-4.4
		0.05	0.50-1.0	12-8	4.5-4.1
25	0.50	0	0.50-1.0	6-10	4.4-4.7
		0.03	0.50-1.0	12-8	5.6-4.5
		0.05	0.50-1.0	12-8	5.1-4.4

The assessed Q values for the best α and β stiffness balances identified in Table 3 are shown in Fig. 19. It is observed that the largest Q values (from 5 to 6.5) are obtained for the models where $\alpha = 0.25$, whereas for the models where $\alpha = 0.50$, Q ranges from 4 to 5.

According to Mexican codes, the largest Q value for the design of ductile systems is $Q = 4$. It can be observed in Tables 4 and 5 that larger values of Q are obtained, particularly for large μ demands on the HEDDs. If one limits $Q \leqslant 4$, the yielding mappings depicted in Fig. 20 are obtained for the models with the best balances. It can be observed that by reducing $Q \leqslant 4$, the system response is much closer to what it was assumed in the design and only incipient yielding of some beams and few columns could develop for an IMRF. From a code-oriented design viewpoint, this is a desirable condition, as one can obtain global ductile performances for a

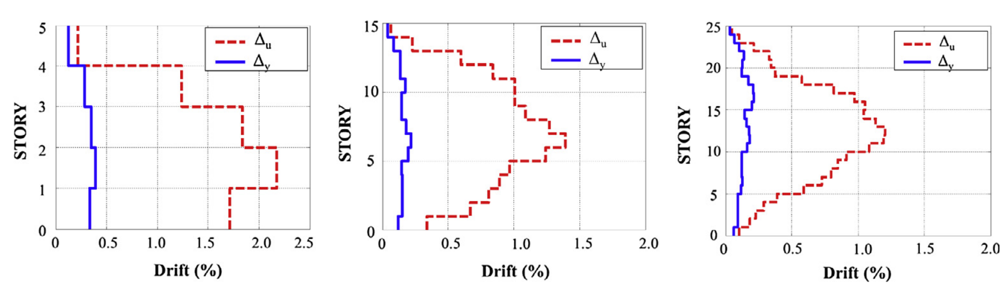

(a) 5-story, α=0.25, β=0.50 (b) 15-story, α=0.25, β=0.50 (c) 25-story, α=0.25, β=0.50

Fig. 18. Story drift envelopes for models where $\theta = 45°$ and $K_2 = 0.05K_{DDE}$.

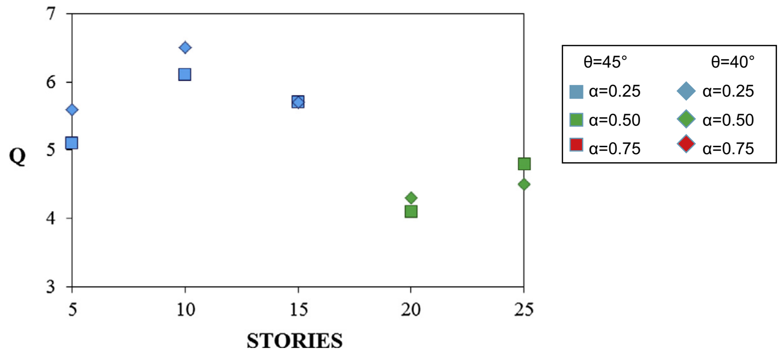

Fig. 19. Seismic response modification factor Q for the best α and β stiffness balances identified in Table 3.

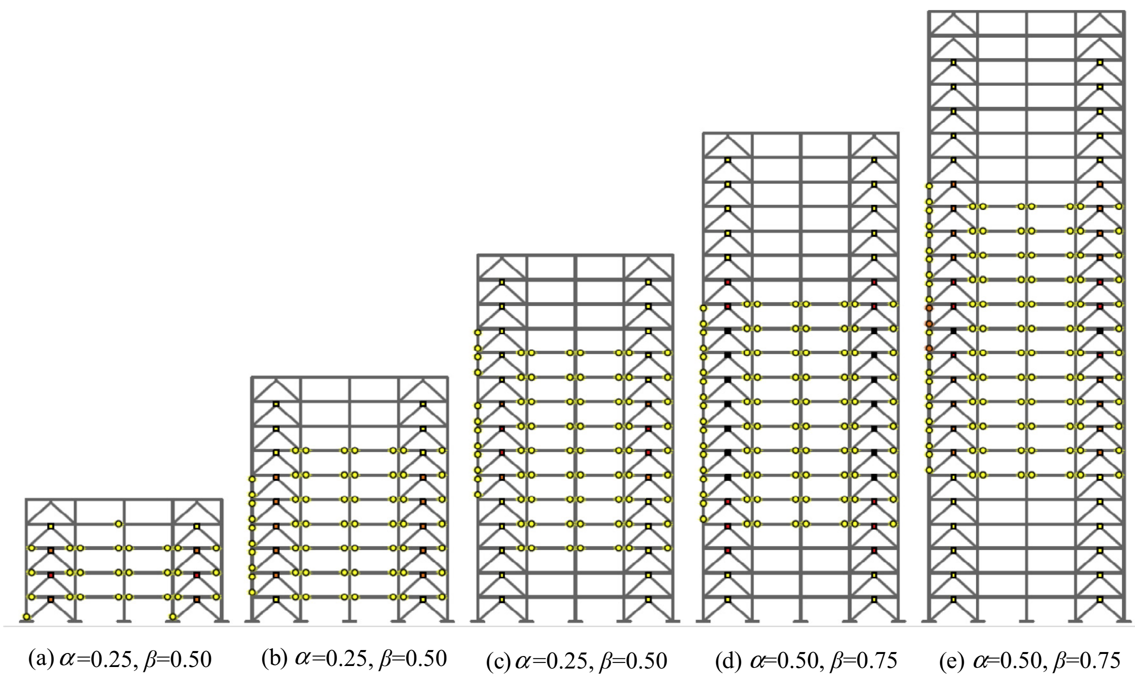

Fig. 20. Inelastic demands mapping when $Q \leqslant 4$ and $\theta = 45°$ and $K_2 = 0.05K_{ELD}$.

non-ductile frame if HEDD are well designed by not abusing of the maximum ductility demands that they can develop.

7.4. Overstrength

Overstrength factors were assessed as $\Omega = V_u/V_{design}$ (Fig. 17), where V_u is the maximum base shear developed by the structural system from pushover analyses and V_{design} is the design base shear for the models (in all cases V_{design} = 0.10 W in this study). Assessed overstrength factors for the best balances (i.e., Fig. 20) are depicted in Fig. 21. For models in the slenderness ratio $0.5 < H/L < 2$, the overstrength factor is $\Omega \approx 1.35$, and for models where $2 < H/L < 3.2$, $\Omega \approx 1.5$.

7.5. Comparison to reference models without HEDDs

In theory, there are two structural systems without HEDDs to directly compare the proposed design method for RC-IMRFs with HEDD: (a) code-designed RC-IMRFs alone and, (b) code-designed RC intermediate moment-resisting braced frames (RC-IMRBFs).

Therefore, in order to compare the proposed structural system with HEDDs to these two structural systems, which Mexican codes allow to design, two additional 15-story models were designed according to current Mexican seismic code guidelines, and assuming the same design base shear $V_{DIS} = V/W = 0.10$: (a) buildings with only RC-IMRFs and, (b) buildings with RC-IMRFs with only chevron braces (RC-IMRBFs) with $\alpha = 0.50$ and $\theta = 45°$.

The obtained results are compared with the best fuse model for that height and α balance: $\alpha = 0.50$, $\beta = 0.75$, $\theta = 45°$, $K_2 = 0.05K_{ELD}$. Pushover analyses were conducted for the resisting frames in the X direction (Fig. 3). To ease the comparison, results are synthesized in Figs. 22–24. The final yielding mappings for each system are shown in Fig. 22, where color codes were explained before. The limits for the buckling shortening of brace sections were defined considering equations derived from experimental research and reported by Kemp [41], as explained in previous research [27,37,42,43]. Resulting normalized global lateral shear vs drift curves (V/V_{DIS} vs Δ) are depicted in Fig. 23. Story drift envelopes at ultimate are shown in Fig. 24.

From the observation of all these figures it is somewhat clear that adding metallic fuses substantially improve the performance of a non-ductile braced framed (RC-IMRBFs) as currently allowed by Mexican codes, as this system has a very low ductility capacity (assessed $Q = 1.8$), considerably smaller than the frame with

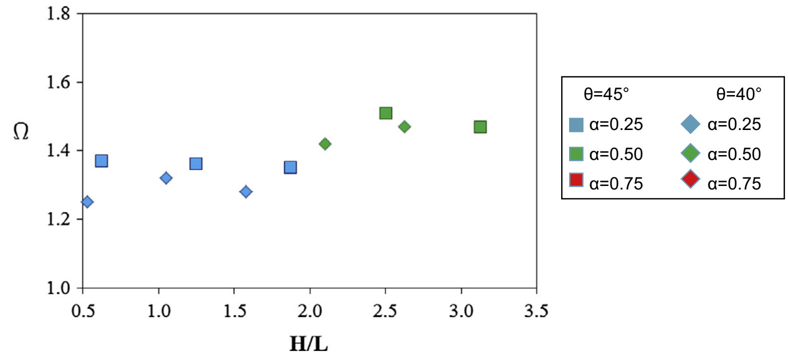

Fig. 21. Overstrength factor assessed for best balances for the best α and β stiffness balances identified in Table 3.

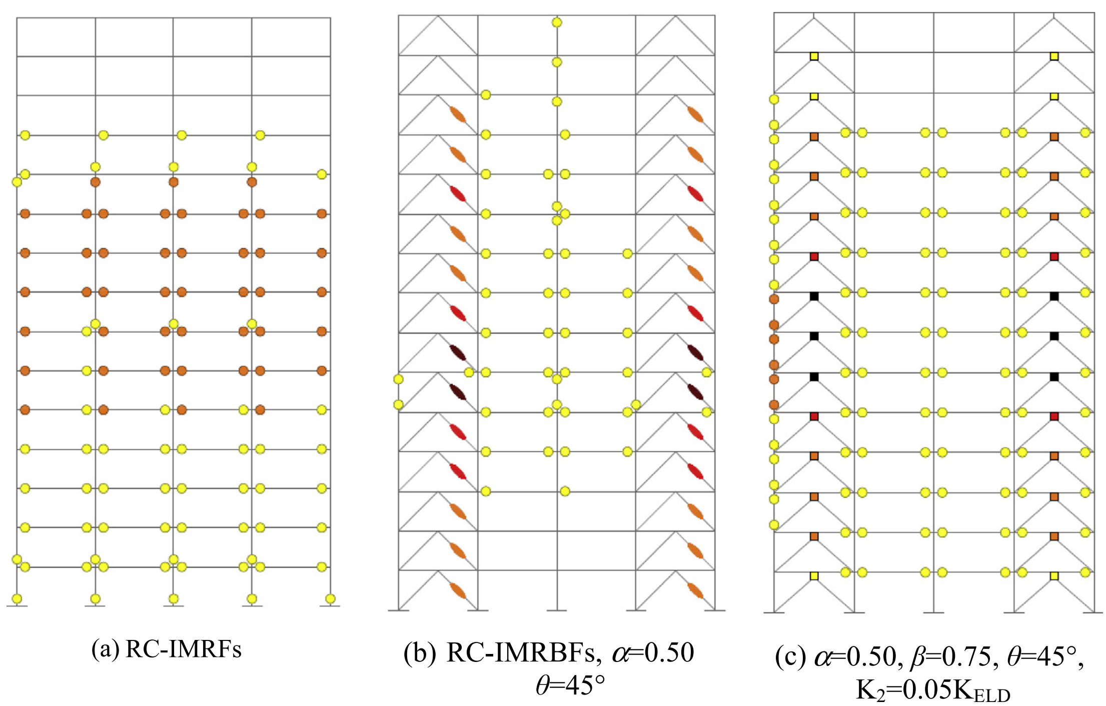

Fig. 22. Inelastic demands mapping for the 15-story models under study.

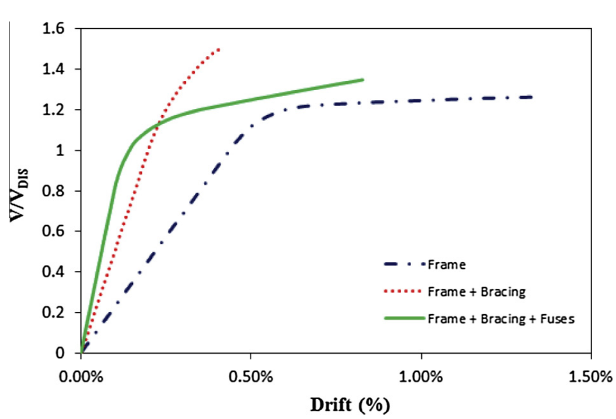

Fig. 23. Normalized global lateral shear vs drift curves for the 15-story models under study.

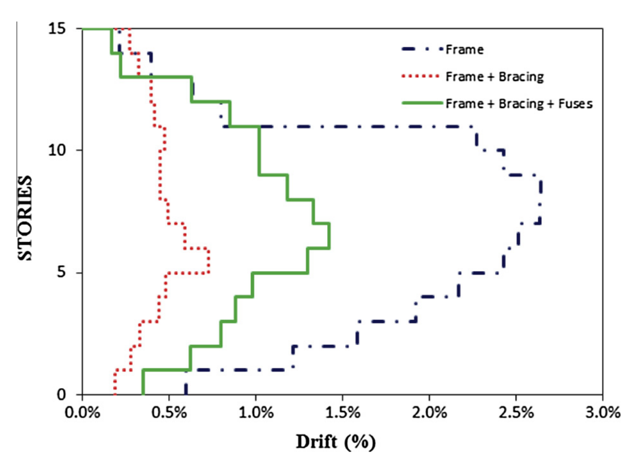

Fig. 24. Story drift envelopes at ultimate for the 15-story models under study.

structural fuses (assessed $Q = 5.6$), although it can develop a relatively higher overstrength, as schematically depicted in Fig. 23. Besides brace buckling, axialization of some exterior and interior columns is also observed where sections are changed (Fig. 22b). As it should be expected, the RC-IMRBF is a rigid system (Fig. 23) that cannot develop large ultimate drifts (Fig. 24).

In agreement with previous studies [44], RC-IMRFs designed according to Mexican codes could develop a decent ductility capacity (assessed $Q = 3.3$). However, the design procedure cannot avoid that some incipient yielding may trigger in some columns, particularly at the stories where sections are changed (Fig. 22a). However, this system developed a smaller ductility and overstrength than the system with structural fuses (Fig. 23) and very large ultimate drifts are required to have such performance (Fig. 24), as the frame system alone is more flexible (Fig. 23).

Therefore, from the analysis of the results that are shown, it can be concluded that for the 15-story models under consideration, the overall performance for the RC-IMRBFs with HEDD is, in theory, a better alternative than the reference systems which structural engineers could currently design under the umbrella of Mexican building codes. There are already proposed design code values for global parameters Q and Ω for these systems in Mexican codes [2].

8. Concluding remarks

Many observations can be done from the extensive and detailed parametric study that was conducted and described in this paper, taking into account that a design base shear V of 10% of the total weight (W) was considered for all models ($V/W = 0.10$).

As observed in a previous parametric study using simple models, the angle of inclination of the chevron braces with respect to the horizontal axis (θ) may be an important variable in the inelastic response of the studied models, even for a variation as small as 5°.

The postyielding stiffness (K_2) of the HEDDs is also important in the inelastic response of such systems. In general, it was observed that the displacement ductility demand (μ) that the HEDDs mounted on chevron braces could develop increases as K_2 increases, particularly when compared to an elastic–perfectly plastic system ($K_2 = 0$). However, the differences observed between $K_2 = 0.03K_{ELD}$ and $K_2 = 0.05K_{ELD}$ were small. The reason is that since K_2 is being directly taken in the design procedure, although elastic–perfectly plastic ($K_2 = 0$) and other bilinear HEDD ($K_2 \neq 0$) are designed to provide the same ultimate maximum force, the resulting yielding force for other bilinear HEDD ($K_2 \neq 0$) is smaller than for the elastic–perfectly plastic HEDD ($K_2 = 0$), so other bilinear HEDD ($K_2 \neq 0$) ended working first in the inelastic range than elastic–perfectly-plastic HEDD.

As expected, as the initial elastic stiffness of the HEDDs gets smaller with respect to the elastic stiffness of the chevron bracing (this is, as β decreases), the ductility (μ) that the HEDDs could develop increases. However, it may also lead to important yielding in beams and columns. In fact, it was observed that if one selects very flexible HEDDs ($\beta = 0.25$), significant inelastic yielding could be developed at exterior corner columns at the stories where the largest values for μ are obtained. Therefore, to minimize the damage potential in columns, $\beta \geqslant 0.5$ according to the studied models. Also, more complex design equations already proposed in the literature to take into account the expected variation on axial force due to the presence of the bracing system (associated to the yielding or buckling of the braces) [43,45] should be explored in future studies, particularly for the design of slender buildings or medium-rise buildings.

Taking into account that the desired design mechanism is the following: strong column-weak beam – strong bracing-weakest HEDD (structural fuse), the best elastic stiffness ratios between the moment frame system and the whole structure (α) were roughly assessed from the inelastic demands mappings. It was observed that for 5–15 story models $\alpha = 0.25$, this is, the largest initial lateral stiffness must be supplied by the bracing-HEDD system. However, as the models became taller (or slender), α should increase, this is, frames must provide a larger initial lateral stiffness (and strength).

It was observed from the inelastic yielding mappings that for most of the studied models, the HEDDs located at the top stories do not yield (elastic response). This observation is not uncommon or new, as it has been reported before in the seismic response of similar buildings with HEDDs where nonlinear dynamic analyses have been performed [46,47]. Therefore, for practical and economical purposes, it is confirmed that in some cases, there is no need to use HEDDs in the last story.

Story drifts related to the first yielding (Δ_y) and to the ultimate limit state (Δ_u) for the complete system were assessed. It was observed that Δ_u increases as: (a) the HEDDs are more flexible (β decreases) and, (b) the postyielding stiffness (K_2) of the HEDDs increases. Δ_u varied from 0.013 to 0.022 for 5 to 15 story models and from 0.012 to 0.015 for 20 to 25 story models. Δ_y varied from 0.002 to 0.004 for 5 to 15 story models and from 0.001 to 0.003 for 20 to 25 story models. An average value for Δ_u and Δ_y cannot be recommended, as they also depend on the combination of relative stiffness parameters α and β, and there is not a single combination that defines the best performance for the models under study.

Overstrength factor Ω tends to increase as α increases (relatively, more participation of the frame). The reason is that whereas the design of the HEDDs is tight, in frame elements (columns and beams), there are strength reserves to satisfy the design objective (strong column-weak beam – strong bracing-weakest HEDD).

The seismic response modification factor Q tends to decrease as the number of stories or slenderness ratio (H/L) increases.

From the results obtained in the reported study, one can conclude that an important global ductility capacity for the whole system (Q in terms of Mexican codes) could be achieved for RC-IMRFs with HEDDs without experiencing important inelastic response in the frame elements (beams and columns) if: (a) $0.25 \leqslant \alpha \leqslant 0.50$, (b) $0.50 \leqslant \beta \leqslant 1.0$ and, (c) $\mu \leqslant 8$, this is, one does not use for design the maximum displacement ductility that HEDDs could develop according to experimental studies.

Also, it can also be concluded that for mid-rise buildings (15 stories), the effect of adding HEDDs help improve the overall seismic performance of RC-IMRF with respect to their two main reference systems: (a) RC-IMRFs only and, (b) RC-IMRFs with chevron braces (RC-IMRBFs). RC-IMRFs with HEDDs develop higher global ductilities than the other reference systems. Beside, this larger ductility capacity is directly related to the yielding of the HEDDs instead of yielding in beams, columns and braces, then satisfying the structural fuse concept. RC-IMRFs alone require of important yielding in beams to achieve an important ductility, whereas RC-IMRBFs cannot achieve important ductilities.

Although the reported parametric study was extensive and comprehensive, additional studies are needed, for example: (a) nonlinear dynamic analyses for records typical of soft and firm soils are needed, (b) the impact of a wider range for the design base shear (V/W) is also important to assess, (c) other structural detailing (ductile confinement for beams and columns) and its impact to the global response, (d) the use of more complex design equations to account for the expected variation on axial force in columns due to the presence of the bracing system and, (e) other structural systems (i.e., steel frames, composite frames, special moment-resisting frames). Some of these variables are currently being evaluated by this research group.

Acknowledgements

The MSc. fellowship granted to the second author by the National Science and Technology Council of Mexico (CONACYT) is gratefully acknowledged. The comments and suggestions of anonymous reviewers were important to improve this paper and are gratefully acknowledged.

References

[1] Tena-Colunga A. State of the art and state of the practice for energy dissipation and seismic isolation of structures in Mexico. In: Proceedings, 10th world conference on seismic isolation, energy dissipation and active vibration control of structures, Istanbul, Turkey, CD-ROM, May; 2007.
[2] NTCS-04. Normas Técnicas Complementarias para Diseño por Sismo. Gaceta Oficial del Distrito Federal, Tomo II, No. 103-BIS, October; 2004 [in Spanish].
[3] MOC-2008. Manual de diseño de obras civiles. Diseño por sismo, Comisión Federal de Electricidad, México, November; 2009 [in Spanish].
[4] Tena-Colunga A, Mena-Hernández U, Pérez-Rocha LE, Avilés J, Ordaz M, Vilar JI. Updated seismic design guidelines for buildings of a model code of Mexico. Earthquake Spectra 2009;25(4):869–98. http://dx.doi.org/10.1193/1.3240413.
[5] ASCE 7. Minimum design loads for buildings and other structures. ASCE Standard ASCE/SEI 7-10, American Society of Civil Engineers, ISBN 0-7844-0809-2; 2010.
[6] Wu J, Hanson RE. Inelastic response of structures with high damping subjected to earthquakes. Report UMCE 87-9. Department of Civil Engineering, The University of Michigan, November; 1987.
[7] Arroyo D, Terán A. Factores de reducción de fuerzas sísmicas para el diseño de estructuras con sistemas pasivos de disipación de energía. Revista de Ingeniería Sísmica 2002;66:73–93 [in Spanish].
[8] Rivera JL, Riddell R, Ruiz SE. Espectros con tasa de falla uniforme para sistemas con disipadores de energía: influencia del índice de daño de Park y Ang. In: Proceedings, XV Congreso Nacional de Ingeniería Estructural, Puerto Vallarta, México, CDROM, 1–12, November; 2006 [in Spanish].
[9] Jara JM, Miranda E, Ayala AG. Parametric study of single-degree-of-freedom systems with energy dissipating devices built on soft soil sites. Eng Struct 2007;29:1398–413. http://dx.doi.org/10.1016/j.engstruct.2006.08.018.
[10] Ruiz SE, Castillo T, Hidalgo JP, Rivera JL. Relación entre la respuesta de S1GDL con amortiguamiento viscoso y la de S1GDL con disipadores de tipo histerético. In: Proceedings, XVI Congreso Nacional de Ingeniería Estructural, Veracruz, México, CDROM, 1–11, November; 2008 [in Spanish].
[11] Ciampi V, Paolone V, De Angelis M. On the seismic design of dissipative bracings. In: Proceedings, tenth world conference on earthquake engineering, Madrid, Spain; 1992. p. 4133–8.
[12] Tsai K-C, Chen H-W, Hong C-P, Su Y-F. Design of steel triangular plate energy absorbers for seismic-resistant construction. Earthquake Spectra 1993;9(3):505–28.
[13] Ciampi V, De Angelis M, Paolone V. Design of yielding or friction-based dissipative bracings for seismic protection of buildings. Eng Struct 1995;17(5):381–91.
[14] Hanson RD, Soong TT. Seismic design with supplemental energy dissipation devices. Monograph Series MNO-8, Earthquake Engineering Research Institute; 2001.
[15] Ruiz SE, Badillo H. Performance-based design approach for seismic rehabilitation of buildings with displacement-dependent dissipators. Earthquake Spectra 2001;17(3):531–48.
[16] Ramírez OM, Constantinou MC, Kircher CA, Whittaker AS, Johnson MW, Gómez JD, et al. Development and evaluation of simplified procedures for analysis and design of buildings with passive energy dissipation systems. Technical Report MCEER-00-0010. Multidisciplinary Center for Earthquake Engineering Research, State University of New York at Buffalo; 2001.
[17] Christopoulos C, Filiatrault A. Principles of passive supplemental damping and seismic isolation. 1st ed. IUSS Press; 2006 [June].
[18] Vargas R, Bruneau M. Analytical investigation of the structural fuse concept. Technical report MCEER-06-004. Multidisciplinary Center for Earthquake Engineering Research, State University of New York at Buffalo; 2006.
[19] Vargas R, Bruneau M. Analytical response and design of buildings with metallic structural fuses. I. ASCE J Struct Eng 2009;135(4):386–93.
[20] Vargas R, Bruneau M. Experimental response of buildings designed with metallic structural fuses. II. ASCE J Struct Eng 2009;135(4):394–403.
[21] Hanson RD. Supplemental damping for improved seismic performance. Earthquake Spectra 1993;9(3):319–34.
[22] Scholl RE. Fundamental design issues for supplemental damping applications. Earthquake Spectra 1993;9(3):627–36.
[23] Symans MD, Charney FA, Whittaker AS, Constantinou MC, Kircher CA, Johnson MW, McNamara RJ. Energy dissipation systems for seismic applications: current practice and recent developments. ASCE J Struct Eng 2008;134(1):3–21.
[24] FEMA-273. NEHRP guidelines for the seismic rehabilitation of buildings. FEMA Publication 273. Washington, DC: Federal Emergency Management Agency, October; 1997.
[25] FEMA-274. NEHRP commentary on the guidelines for the seismic rehabilitation of buildings. FEMA Publication 274. Washington, DC: Federal Emergency Management Agency, October; 1997.
[26] Tena-Colunga A, Correa-Arizmendi H, Luna-Arroyo JL, Gatica-Avilés G. Seismic behavior of code-designed medium rise special moment-resisting frame RC buildings in soft soils of Mexico City. Eng Struct 2008;30(12):3681–707. http://dx.doi.org/10.1016/j.engstruct.2008.05.026.
[27] Godínez-Domínguez EA, Tena-Colunga A, Pérez-Rocha LE. Case studies on the seismic behavior of reinforced concrete chevron braced framed buildings. Eng Struct 2012;45(12):78–103. http://dx.doi.org/10.1016/j.engstruct.2012.05.005.
[28] Tena-Colunga A. Some aspects on the analytical modelling of metallic energy dissipation devices. In: Proceedings, 12th European conference on earthquake engineering, London, England, CD-ROM, Paper No. 060, September; 2002.
[29] Nangullasmú HJ. Propuesta de criterios de diseño sísmico conforme a reglamento para marcos no dúctiles de concreto reforzado con disipadores histeréticos. MSc. Thesis, Posgrado en Ingeniería Estructural, División de Ciencias Básicas e Ingeniería, Universidad Autónoma Metropolitana Azcapotzalco, December; 2011 [in Spanish].
[30] Martínez-Romero E. Experiences on the use of supplementary energy dissipators on building structures. Earthquake Spectra 1993;9(3):581–626.
[31] Whittaker A, Bertero VV, Thompson C, Alonso J. Earthquake simulator testing of steel plate added damping and stiffness elements. Report UCB/EERC-89/02. Earthquake Engineering Research Center, University of California at Berkeley; 1989.
[32] Aguirre M, Sánchez R. Structural seismic damper. ASCE J Struct Eng 1992;118(5):1158–71.
[33] Tena-Colunga A, Nangullasmú-Hernández HJ. Diseño sísmico de marcos no dúctiles de concreto reforzado con disipadores de energía histeréticos. Definición de parámetros de diseño. Revista Internacional de Desastres Naturales, Accidentes e Infraestructura Civil 2013;13(2):275–99 [in Spanish].
[34] Tena-Colunga A. Mathematical modelling of the ADAS energy dissipation device. Eng Struct 1997;19(10):811–21.
[35] NTCC-2004. Normas Técnicas Complementarias para Diseño y Construcción de Estructuras de Concreto. Gaceta Oficial del Distrito Federal, México, October; 2004 [in Spanish].
[36] ACI-318-11. Building code requirements for structural concrete (ACI-318-11) and commentary (ACI 318R-11). American Concrete Institute, Farmington Hills, Michigan, USA; 2011.
[37] Godínez-Domínguez EA. Estudio del comportamiento de marcos dúctiles de concreto reforzado con contraventeo chevrón. Ph.D. thesis, División de Ciencias Básicas e Ingeniería, Universidad Autónoma Metropolitana Azcapotzalco, July; 2010 [in Spanish].
[38] Godínez EA, Tena A. Efecto de los modos superiores en la respuesta no lineal de marcos dúctiles de concreto reforzado con contraventeo metálico tipo chevrón. Caso de estudio. Revista Internacional de Ingeniería de Estructuras 2014;19(2):171–81 [in Spanish].
[39] Chopra AK, Goel RK. A modal pushover analysis for estimating seismic demands of buildings. Earthquake Eng Struct Dynam 2002;31:561–82.
[40] Goel RK, Chopra AK. Evaluation of modal and FEMA pushover analyses: SAC Buildings. Earthquake Spectra 2004;20(1):225–54.
[41] Kemp RA. Inelastic local and lateral buckling in design codes. ASCE J Struct Eng 1996;122(4):374–82.
[42] Godínez-Domínguez EA, Tena-Colunga A. Nonlinear behavior of code-designed reinforced concrete concentric braced frames under lateral loading. Eng Struct 2010;32:944–63. http://dx.doi.org/10.1016/j.engstruct.2009.12.020.
[43] Tapia-Hernández E, Tena-Colunga A. Code-oriented methodology for the seismic design of regular steel moment resisting braced frames. Earthquake Spectra 2014;30(4):1683–709. http://dx.doi.org/10.1193/032012EQS100M.
[44] Tena-Colunga A, Gatica-Avilés G, Urbina-Californias LA, Victoria-Torres L. Impacto de la disposición de vigas secundarias en losas perimetralmente apoyadas en el comportamiento sísmico de edificios diseñados con base en marcos de concreto reforzado. Revista Internacional de Ingeniería de Estructuras 2012;17(1 and 2):63–85 [in Spanish].
[45] Lacerte M, Tremblay R. Making use of brace overstrength to improve the seismic response of multistory split-X concentrically braced steel frames. Can J Civ Eng 2006;33:1005–21.
[46] Tena-Colunga A, Del Valle Calderón E, Pérez-Moreno D. Issues on the seismic retrofit of a building near resonant response and structural pounding. Earthquake Spectra 1996;12(3):567–97.
[47] Tena-Colunga A, Vergara A. Comparative study on the seismic retrofit of a mid-rise steel building: steel bracing vs energy dissipation. Earthquake Eng Struct Dynam 1997;26(6):637–45. June..